arXiv:1701.04859v1 [astro-ph.SR] 17 Jan 2017

A proper motions study of the globular cluster NGC 3201.[1]

Devesh P. Sariya[1], Ing-Guey Jiang[1], R. K. S. Yadav[2]
[1]*Department of Physics and Institute of Astronomy, National Tsing-Hua University, Hsin-Chu, Taiwan*
email: deveshpath@gmail.com
[2]*Aryabhatta Research Institute of Observational Sciences, Manora Peak, Nainital 263 002, India*

ABSTRACT

With a high value of heliocentric radial velocity, a retrograde orbit, and being suspected to have an extragalactic origin, NGC 3201 is an interesting globular cluster for kinematical studies. Our purpose is to calculate the relative proper motions (PMs) and membership probability for the stars in the wide region of globular cluster NGC 3201. Proper motion based membership probabilities are used to isolate the cluster sample from the field stars. The membership catalogue will help address the question of chemical inhomogeneity in the cluster. Archive CCD data taken with a wide-field imager (WFI) mounted on the ESO **2.2**m telescope are reduced using the high-precision astrometric software developed by Anderson et al. for the WFI images. The epoch gap between the two observational runs is ∼14.3 years. To standardize the BVI photometry, Stetson's secondary standard stars are used. The CCD data with an epoch gap of ∼14.3 years enables us to decontaminate the cluster stars from field stars efficiently. The median precision of PMs is better than ∼0.8 mas yr^{-1} for stars having V <18 mag that increases up to ∼1.5 mas yr^{-1} for stars with $18 < V < 20$ mag. Kinematic membership probabilities are calculated using proper motions for stars brighter than V ∼20 mag. An electronic catalogue of positions, relative PMs, BVI magnitudes and membership probabilities in ∼19.7×17 arcmin^2 region of NGC 3201 is presented. We use our membership catalogue to identify probable cluster members among the known variables and X-ray sources in the direction of NGC 3201.

Subject headings: Galaxy: Globular cluster: individual: NGC 3201 - astrometry - catalogs

1. Introduction

Galactic globular clusters are very important for the study of the halo and bulge regions of our Galaxy. In particular, they are the best tools to understand the kinematics and dynamics of the halo region of the Milky Way by the virtue of being easily distinguishable at large distances (Cudworth 1997, Dambis 2006). Since the emergence of CCDs, proper motion (PM) studies can be carried out with unprecedented precision using CCD data with smaller epoch differences than data from photographic plates. Proper motions are the root to learn about the kinematics and orbit of the clusters as well as providing kinematical membership probabilities of the stars. Membership status is often pivotal to spectroscopic studies, to avoid observing field stars lying in the cluster's field (Cudworth 1986). At fainter magnitudes, in particular, field stars dominate, and proper motions become very important in removing them from the sample (Piotto et al. 2004).

NGC 3201 is a sparse, metal-poor, intermediate-mass halo globular cluster. The basic cluster parameters of NGC 3201 taken from Harris (1996, 2010 edition) are listed in Table 1. Since the cluster is less centrally concentrated than most other

[1]Based on observations with the MPG/ESO 2.2m and ESO/VLT telescopes, located at La Silla and Paranal Observatory, Chile, under DDT programs 164.O-0561(F), 093.A-9028(A) and the archive material.

globular clusters, even ground based telescopes can probe its central region. Due to this advantage and its proximity, NGC 3201 has been studied extensively for photometric studies (Menzies 1967, Alcaino 1976, Lee 1977, Alcaino et al. 1981,1989, Cacciari 1984a, 1984b, Penny 1984, Brewer et al. 1993, Covino & Ortolani 1997, Kravtsov et al. 2009 etc.). von Braun & Mateo (2001) presented an extinction map for NGC 3201 and explained that due to its low Galactic latitude, the effect of differential reddening across this globular cluster is very significant. NGC 3201 has been studied for the question of chemical abundances and possibility of inhomogeneity in its stellar population by several authors (e.g., Chun 1988, Gonzalez & Wallerstein 1998, Covey et al. 2003, Kravtsov et al. 2010, Simmerer et al. 2013, Muñoz et al. 2013, Mucciarelli et al. 2015 and references therein). NGC 3201 is known to harbor many variable stars including RR Lyrae, SX Phoenicis etc. It belongs to Oosterhoff type I according to Oosterhoff dichotomy of RR Lyrae Stars. The cluster has been the subject of many investigations for searching and characterizing its variable stars (e.g., Lee & Carney 1999, von Braun & Mateo 2002, Piersimoni et al. 2002, Mazur et al. 2003, Layden et al. 2003, Arellano Ferro et al. 2014, Kaluzny et al. 2016 and references therein). Webb et al. (2006) studied NGC 3201 using $XMM-Newton$ X-ray observatory.

NGC 3201 is a very interesting globular cluster for its kinematical features. It shows a very high value of heliocentric radial velocity (494.2 km/sec, Cote et al. 1994) suggesting a retrograde orbit about the Galactic center (Casetti-Dinescu et al. 2007). It has been suspected to have an extragalactic origin and has probably been accreted by the Milky Way. Dynamics of the cluster was studied by Da Costa et al. (1993) and Cote et al. (1994, 1995). The Radial Velocity Experiment (RAVE) catalogue was used to study this cluster by Kunder et al. (2014) and Anguiano et al. (2015, 2016). Anguiano et al. (2016) presented the distribution of stars based on UCAC4 proper motions. Chen & Chen (2010) state that NGC 3201 appears to have passed through the Galactic disk a few Myr ago and the cluster has clumps along its Galactic north-south axis.

Casetti-Dinescu et al. (2007) provided the absolute proper motion of NGC 3201 ($\mu_\alpha cos\delta$ = 5.28 ± 0.32 mas yr^{-1}, $\mu_\delta = -0.98 \pm 0.33$ mas yr^{-1}) using a combination of photographic plate data with CCD. Recently, Zloczewski et al. (2012) (hereafter, Zl12) have determined proper motions for the stars in the region of NGC 3201 and provided membership probabilities in the central region of the cluster.

From the above discussion, it is noticeable that this kinematically interesting globular cluster is not well studied for proper motions over a wider region. As reported by Brewer et al. (1993) and Kravtsov et al. (2009), the studies of NGC 3201 are obstructed by significant field star contamination. Wide Field Imagers (WFIs) enable us to cover the broad regions of star clusters, sometimes up to their tidal trails. The archive data observed with WFI@2.2m at La Silla, Chile has been used previously to provide proper motions using a time gap of a few years (Anderson et al. 2006; Yadav et al. 2008, 2013; Bellini et al. 2009; Sariya et al. 2012, 2015). NGC 3201, being a sparse cluster and the available epoch gap being ∼14.3 years in the archive data of WFI@2.2M allows us to determine precise proper motions over a broad region of the cluster.

The main goal of the present article is to provide relative PMs and membership probabilities (P_μ) for stars having visual magnitudes up to 20 mag in the wide field of NGC 3201. We also provide an electronic catalogue for 8322 stars which contains B, V, I magnitudes, PMs and membership probabilities for the follow-up studies of the cluster. Our membership catalogue covers a region of ∼19.7×17 arcmin^2 which is wider than the area covered in the PM study by Zl12 (∼14.6×9.7 arcmin^2). Our membership catalogue will be helpful to select the more likely cluster members while addressing the question of chemical inhomogeneity which has been an intriguing aspect of this cluster.

Information about the data used and reduction procedures are described in Section 2 where we also discuss PMs, vector point diagrams (VPDs) with color-magnitude diagram (CMD) of the cluster. Cluster membership analysis is provided in Section 3. We use our membership catalogue to examine the membership status of earlier reported variables and X-ray sources in Section 4. The electronic catalogue being presented for the further studies of the cluster is explained in Section 5. Conclusions follow in Section 6.

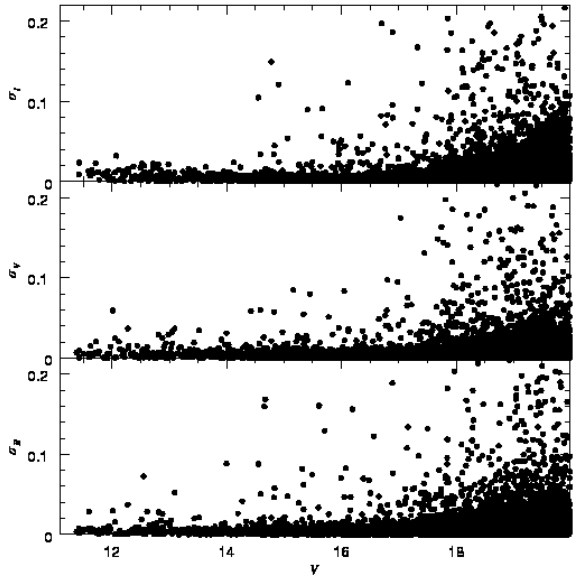

Fig. 1.— Plot of the rms of the residuals around the mean B, V, and I magnitudes, for stars in the NGC 3201 field imaged in this study, plotted against V magnitude

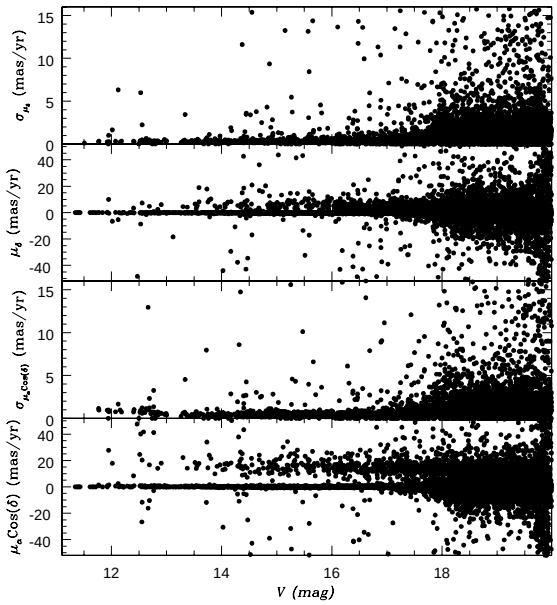

Fig. 2.— Proper motions of stars in the NGC 3201 field, in the globular cluster reference frame. Proper motions in RA and Dec are plotted against V magnitude, along with their rms errors

.

Table 1: Basic parameters of NGC 3201 taken from Harris (1996, 2010 edition). The notations used have their usual meanings. Cluster's heliocentric distance is denoted by d and the Galactocentric distance is denoted by R_{GC}.

Parameters	Values
α_{2000}	$10^{\rm h}\ 17^{\rm m}\ 36^{\rm s}.82$
δ_{2000}	$-46^\circ\ 24'\ 44.9''$
l	$277\overset{\circ}{.}23$
b	$8\overset{\circ}{.}64$
[Fe/H]	-1.59
$E(B-V)$	0.24 mag
d	4.9 kpc
R_{GC}	8.8 kpc

Table 2: Details of the WFI@**2.2**m archive data. The first epoch data were acquired on December 05, 1999 and the second epoch data were taken between April 02-05, 2014.

Filters	Exposure time (seconds)	Seeing (arcsec)	Airmass
December 05, 1999 (First epoch)			
B	2×240	1.1	∼1.3
V	2×240	0.9	∼1.3
I	2×240	0.8	∼1.2
April 02-05, 2014 (Second Epoch)			
V	35×40	1.1	∼1.1

2. Data used and reduction procedures

To determine the PMs of the stars in this work, we used archive images[2] from observations made with the 2.2m ESO/MPI telescope at La Silla, Chile. This telescope contains a mosaic camera called the Wide-Field Imager (WFI), consisting of 4×2, i.e. 8 CCD chips. Since each CCD has an array of 2048×4096 pixels, WFI ultimately produces images with a 34×33 arcmin^2 field of view.

Table 2 presents the details of the observational log of the archive data. The observational run of the first epoch contain 2 images in B, V and I bands each with 240 sec exposure time observed on December 05, 1999. In the second epoch, we have 35 images with 40 sec exposure time each in V filter observed between April 02−05, 2014. Thus, the epoch gap between the data is ∼14.3 years. As can be seen in the Table 2, seeing in the images used are 0.8–1.1 arcsec, and airmass values lie between ∼ 1.1–1.3.

2.1. The data reduction procedures

To derive PMs from the WFI@2.2m mosaic CCD images, we used the astrometric procedure developed by Anderson et al. (2006, hereafter A06). The technique involves the usual initial steps of de-biasing and flat-fielding. One of the decisive factors in providing precise positions of the stars is constructing a good Point Spread Function (PSF) for the WFI images. Since the shape of the PSF changes across the mosaic CCD, we capture this variability by using an array of 15 PSFs per CCD chip (3 across and 5 high), as explained in A06. To furnish positions and fluxes of the objects in an image, an array of *empirical* PSFs are constructed. These PSFs are saved in a look-up table on a very fine grid of a quarter pixel size. Each PSF goes out to a radius of 25 pixels and each pixel is split in 4 equal parts, thus giving (201, 201) grid points for a PSF. The center of the PSF is located at the central gridpoint (101, 101). A06 presented the automated code we are now using to iteratively determine the precise positions and instrumental magnitudes for the brightest down to faintest stars for B, V, I bands.

As documented in A06, WFI@**2.2**m is affected by significant geometric distortion in the focal plane, which leads the pixel scale across the field-of-view to change effectively. The corrections to account for the geometric distortion were derived using dithered observations of Baade's window which lies in the Galactic bulge (see, A06). The corrections have been noted in a look-up table comprising 9×17 elements, for each chip. For any particular location, a bi-linear interpolation between the four closest grid points from the look-up table to the target point delivers the distortion correction. Still, the distortion may vary over time for the WFI, and is typically larger near the edges of the image. These factors lead to uncertainty in distortion corrections. To tackle this uncertainly, we followed the local transformation approach as described in Section 7 of the article A06. According to the local transformation approach, transformations from one frame to another are obtained locally, i.e. with respect to some stars in our own images. Because cluster stars exhibit lesser amount of internal dispersion than the field stars, cluster stars based on their location in CMD and motion are chosen as reference. Initially, we choose stars lying on the main sequence, sub giant and red giant branches by making blue and red envelope for the sequences in the CMD. In subsequent attempts, the selection is done using PMs. The process is iterated multiple times to provide the best possible results. After positions of stars are determined in all frames, we use six-parameter linear transformations to transform the positions from one frame to another. This approach resembles the classical "plate-pair" method (e.g., Sanders 1971a, Tian et al. 1998), but it is more generalized and can be used to all possible combinations of the first and second epoch frames. The relative PM of a target star will be the average of all displacements for inter epoch transformations. Since PMs do not contribute to the intra-epoch displacements, they are used to calculate errors in PM measurements.

2.1.1. Calibrating the photometry

Instrumental B, V and I magnitudes were transformed into standard Johnson–Cousin system using secondary standard stars provided by P. Stetson[3]. The standard stars used for calibra-

[2] http://archive.eso.org/eso/eso_archive_main.html

[3] http://www3.cadc-ccda.hia-iha.nrc-cnrc.gc.ca/community/STETSON/standards/

tion have a brightness range of $12.6 \leq V \leq 19.8$ and color ranges of $0.4 \leq (B-V) \leq 1.5$ and $0.4 \leq (V-I) \leq 1.9$. A total of 160 stars for BV magnitudes and 165 stars for I magnitudes were used in the calibration process.

We used the transformation equations written below to derive the photometric zero-points and color terms:

$$B_{\rm std} = B_{\rm ins} + C_b \times (B_{\rm ins} - V_{\rm ins}) + Z_b$$
$$V_{\rm std} = V_{\rm ins} + C_v \times (B_{\rm ins} - V_{\rm ins}) + Z_v$$
$$I_{\rm std} = I_{\rm ins} + C_i \times (V_{\rm ins} - I_{\rm ins}) + Z_i,$$

where instrumental magnitudes and secondary standard magnitudes have been denoted by subscripts "ins" and "std" respectively. C_b, C_v and C_i denote the color terms, while Z_b, Z_v and Z_i are the global zero-points. As a result of the calibration, the values of the color-terms are 0.39, -0.07 and 0.12, whereas the zero-points are 24.79, 24.18, 23.27 for B, V and I filters respectively. These values of color terms and zero-point agree with the values posted on the WFI@**2.2**m webpage[4].

The photometric standard deviations for individual photometric bands were calculated by reducing multiple observations to a common reference frame. Figure 1 presents the rms error in the magnitudes for B, V and I magnitudes as a function of visual magnitude. The values of average rms are less than $\sim$0.01 mag for stars brighter than 19 mag for B and I filters and better than $\sim$0.01 mag for $V < 20$ mag.

2.1.2. Calibrating the positions

As a part of the astrometric studies of NGC 3201, we present the equatorial coordinates of stars in International Celestial Reference System (ICRS). We used the geometric distortion correction from the look-up table given in the A06 to correct the pixel coordinates X, Y of each star in each frame and averaged by means of a six parameter linear transformation into a common reference frame. The online digitized sky ESO catalogue in the SKYCAT software is then used to transform the averaged X, Y positions to right ascension (RA) and declination (Dec) in J2000.0 equinox using IRAF[5] tasks *CCMAP* and *CCTRAN*. The transformations have rms values of about $\sim$ 20 mas. The relatively high accuracy of our distortion corrections as well as the reasonable stability of the intra-chip positions makes it possible to apply a single plate model which includes linear and quadratic terms and a small but significant cubic term in each coordinate. Also, this solution removes the effects caused by differential refraction.

2.2. Proper motion determinations

We used 6 images from the first epoch and 35 images from the second epoch to determine PMs for NGC 3201 stars. Having a large number of images minimizes the value of the standard error in the PMs.

We started with a selection of photometric clusters members, i.e. members selected on the basis of their position in V vs $(B-V)$ CMD. We selected stars lying near the cluster sequences in the CMD, with brightness in the range of $14 \leq V \leq 19$. These are used as a local reference to transform the coordinates of the stars between the epochs. Adopting only those stars lying on the cluster sequences in the CMD and having PM errors $<$1.0 mas yr^{-1} ensure that the PMs are determined with respect to the systematic motion of the cluster. To minimize the influence of uncorrected geometric distortion residuals, a local transformation based on the closest 25 reference stars on the same CCD chip was used. We did not find any systematics larger than random errors close to the corners or edges of the CCD chips.

The routine described in A06 has an iterative nature and we iterated it to remove some stars from the initial photometric member list. Stars were eliminated if they had PMs inconsistent with cluster membership, in spite of their colors placing them near the cluster sequence in the CMD. PMs and their rms errors are plotted as a function of visual magnitude in Figure 2. The median value of PM error is $\sim$0.8 mas yr^{-1} for stars brighter than $V \sim$18 mag which increases up to $\sim$1.5 mas yr^{-1} for stars in the magnitude range of $18 < V < 20$ mag.

[4] http://www.ls.eso.org/lasilla/sciops/2p2/E2p2M/WFI/zeropoints/

[5] IRAF is distributed by the National Optical Astronomical Observatory which is operated by the Association of Universities for Research in Astronomy, under contact with the National Science Foundation

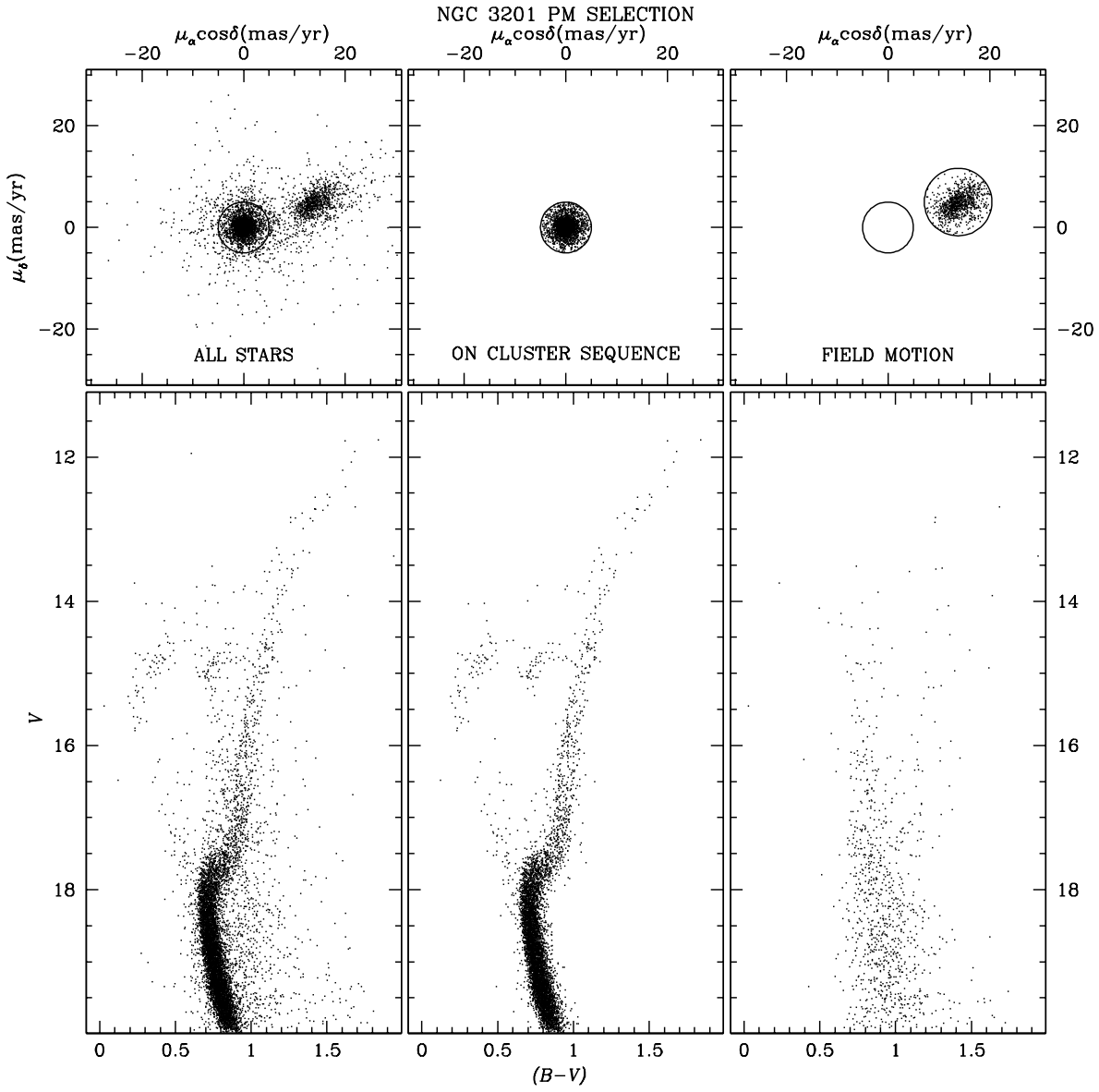

Fig. 3.— *(Top panels)* Proper motion vector-point diagrams (VPDs). Zero point in VPD is the average motion of the assumed cluster stars. *(Bottom panels)* V vs. $(B-V)$ CMDs. *(Left)* The whole sample; *(center)* stars in VPD within ∼5 mas yr^{-1} around the cluster mean motion. *(Right)* Probable field stars in the region of NGC 3201. For all the plots only stars having PM error better than 2 mas yr^{-1} in each coordinate have been considered.

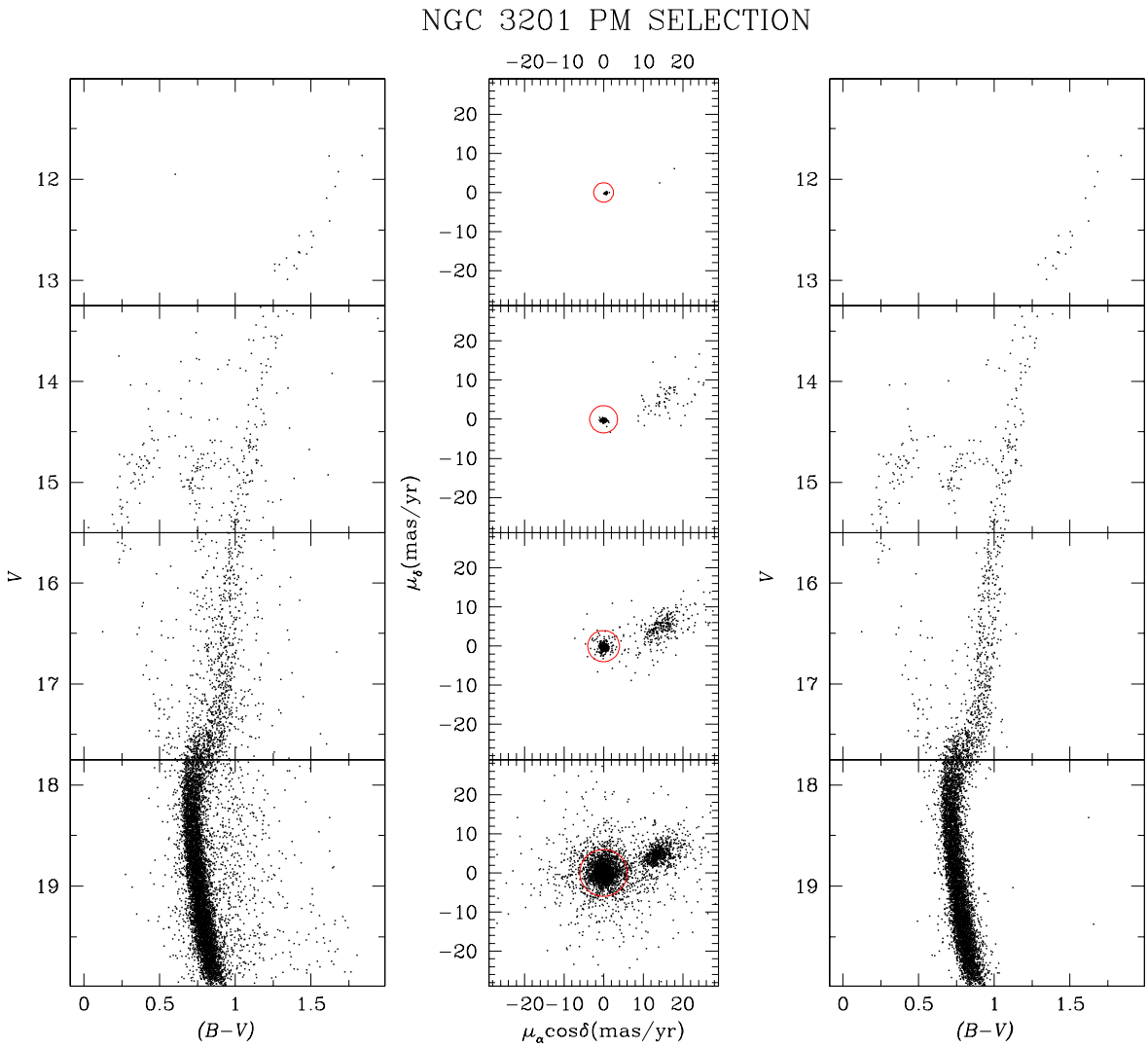

Fig. 4.— *(Left:)* Magnitude-binned CMD of the stars while PM errors increase from 1.2 mas yr^{-1} for the brightest bin to 2.5 mas yr^{-1} for the faintest bin. *(Middle:)* VPDs for the same stars lying in the corresponding magnitude bins. A circle in each VPD shows the adopted membership criterion. The radii of the circles increase from 2.5 mas yr^{-1} to 6.0 mas yr^{-1} from bright to fainter bins. *(Right:)* CMD for stars expected to be cluster members.

2.2.1. Cluster CMD decontamination

One of the main reasons to carry out PM analysis for star clusters is to isolate the cluster sample from the field stars and to produce a CMD with only the most probable cluster members. Figure 3 clearly demonstrates the strength of PM analysis in separating the field stars using vector-point diagrams (VPDs) in the top panels, in combination with V versus $(B-V)$ CMDs in the bottom panels. In the left panels of the figure, the entire sample of stars is shown, while the middle panels and right panels represent likely cluster members and field stars respectively. In the top middle panel, VPD has a circle of radius $\sim$5 mas yr^{-1} around the cluster centroid. This motion circle is our provisional criterion for assigning membership to the stars, before membership probabilities are determined. The radius of the circle is chosen as a compromise between losing cluster members with poorly measured PMs and including some field stars that have their PMs consistent with the cluster's mean PM. The shape of the cluster members' PM distribution in the VPD is round, which suggests that our PM measurements are not affected by any systematics. It is pretty obvious from the figure that having a large epoch gap for CCD data has produced a CMD almost free from field stars.

Figure 4 shows the $(B-V), V$ CMD which is binned along the magnitude axis. To identify provisional cluster members, different selection criteria were used in different magnitude bins. The criterion was tighter for bright stars as they have more reliable measurements, but is less stringent for fainter stars. As can be seen in Figure 4, fainter stars have poorer PM determinations compared to brighter stars: PM uncertainty increases from 1.2 mas yr^{-1} to 2.5 mas yr^{-1} from the brightest bin to the faintest one. We therefore adopt a PM selection radius that increases from 2.5 mas yr^{-1} in the brightest magnitude bin to 6.0 mas yr^{-1} in the faintest one. However, we still have a good enough decontamination of field stars even in the fainter magnitudes.

3. Membership probabilities

In Figure 3, two different groups of stars are distinguishable based on their motion, although a larger fraction of the stars are inside the circle for provisional cluster membership. The next step is to determine membership probabilities of stars which will yield a quantitative significant number for a particular star belonging to the cluster. The credit to set up a mathematical model to use PMs to determine membership probabilities goes to Vasilevskis et al. (1958). The maximum likelihood principle to compute membership probabilities was introduced by Sanders (1971b). Over the years, methods to calculate membership probabilities have been refined (e.g., Stetson 1980; Zhao & He 1990; Zhao & Shao 1994). In this study, we use the method given by Balaguer-Núñez et al. (1998). This method has been previously used for both globular clusters (Bellini et al. 2009, Sariya et al. 2012, 2015) and open clusters (Yadav et al. 2013). According to this method, two frequency distribution functions are constructed for a particular ith star. Frequency distributions of cluster stars (ϕ_c^ν) and field stars (ϕ_f^ν) are presented by the equations given below:

$$\phi_c^\nu = \frac{1}{2\pi\sqrt{(\sigma_c^2+\epsilon_{xi}^2)(\sigma_c^2+\epsilon_{yi}^2)}} \times \exp\{-\frac{1}{2}[\frac{(\mu_{xi}-\mu_{xc})^2}{\sigma_c^2+\epsilon_{xi}^2} + \frac{(\mu_{yi}-\mu_{yc})^2}{\sigma_c^2+\epsilon_{yi}^2}]\}$$

and

$$\phi_f^\nu = \frac{1}{2\pi\sqrt{(1-\gamma^2)}\sqrt{(\sigma_{xf}^2+\epsilon_{xi}^2)(\sigma_{yf}^2+\epsilon_{yi}^2)}} \times \exp\{-\frac{1}{2(1-\gamma^2)}[\frac{(\mu_{xi}-\mu_{xf})^2}{\sigma_{xf}^2+\epsilon_{xi}^2} - \frac{2\gamma(\mu_{xi}-\mu_{xf})(\mu_{yi}-\mu_{yf})}{\sqrt{(\sigma_{xf}^2+\epsilon_{xi}^2)(\sigma_{yf}^2+\epsilon_{yi}^2)}} + \frac{(\mu_{yi}-\mu_{yf})^2}{\sigma_{yf}^2+\epsilon_{yi}^2}]\}$$

where (μ_{xi}, μ_{yi}) are the PMs of i^{th} star, while (ϵ_{xi}, ϵ_{yi}) are the proper motion errors. (μ_{xc}, μ_{yc}) represent the cluster's PM center and (μ_{xf}, μ_{yf}) are the field PM center. For the cluster members, the intrinsic proper motion dispersion is denoted by σ_c, whereas σ_{xf} and σ_{yf} exhibit the field intrinsic proper motion dispersions. The correlation coefficient γ is calculated as:

$$\gamma = \frac{(\mu_{xi}-\mu_{xf})(\mu_{yi}-\mu_{yf})}{\sigma_{xf}\sigma_{yf}}.$$

The spatial distribution of the stars was not considered in calculating membership. In computing ϕ_c^ν and ϕ_f^ν, we used those stars which have PM errors better than $\sim$2 mas yr^{-1}. In

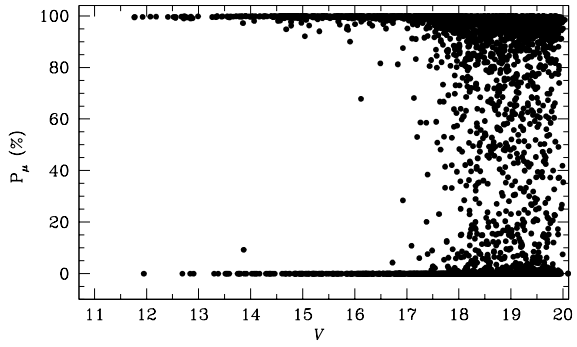

Fig. 5.— Membership probability $P_\mu(\%)$ of the stars in the direction of NGC 3201 plotted as a function of the V magnitude. For stars having magnitudes $V \sim 18$ mag and fainter, the average P_μ are decreasing for cluster members, while they are increasing for field stars.

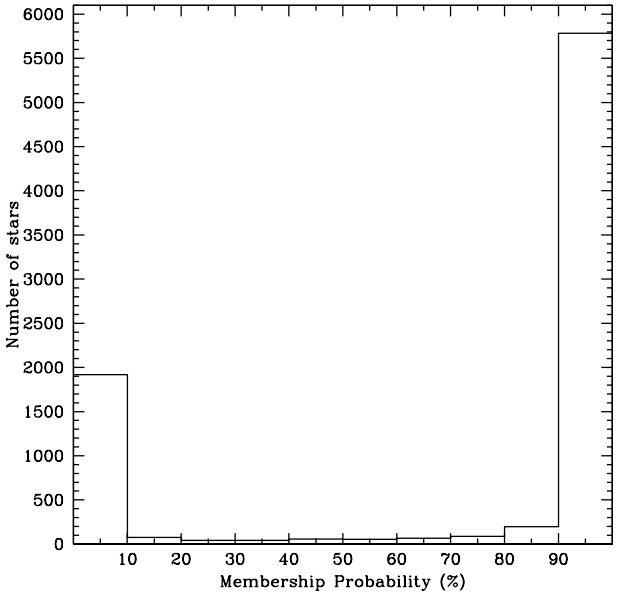

Fig. 6.— Histogram of the membership probabilities derived in this study.

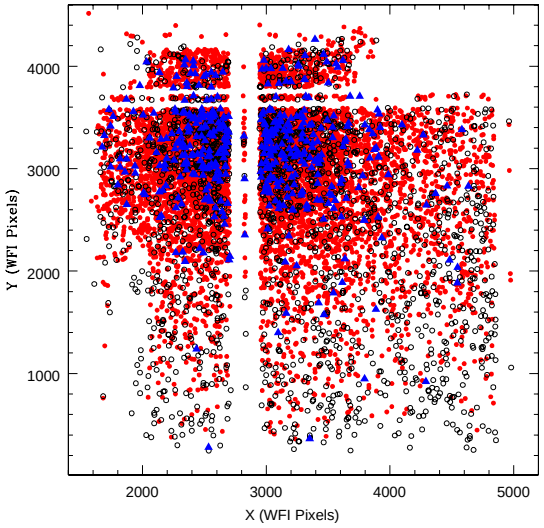

Fig. 7.— Spatial distribution of stars presented in this study. Red filled circles are the stars with $P_\mu > 80\%$, blue triangles show the stars having $10\% < P_\mu \leq 80\%$, and black open circles show the stars with $P_\mu \leq 10\%$. Stars having proper motion error better than 2 mas yr^{-1} are plotted here. The gaps which form a "cross" like pattern are due to the gaps in the mosaic CCD system.

VPD, the center of the cluster stars is found to be (μ_{xc}, μ_{yc})=(0, 0) mas yr^{-1}. The intrinsic PM dispersion for the cluster stars (σ_c) could not be ascertained reliably using our PM data. Pryor & Meylan (1993) list the value of radial velocity dispersion for NGC 3201 as 5.2 km sec^{-1}. Considering the value of the distance of NGC 3201 as 4.9 kpc (Harris 1996, 2010 edition), the internal PM dispersion becomes ∼0.22 mas yr^{-1}. Hence, we used σ_c= 0.22 mas yr^{-1}. For field stars, we have (μ_{xf}, μ_{yf}) = (13.8, 4.8) mas yr^{-1} and (σ_{xf}, σ_{yf}) = (2.5, 2.1) mas yr^{-1}.

If n_c and n_f are the normalized number of cluster and field stars respectively (i.e., $n_c + n_f = 1$), the total distribution function can be calculated as:

$$\phi = (n_c \times \phi_c^{\nu}) + (n_f \times \phi_f^{\nu}),$$

As a result, the membership probability for the i^{th} star is given by:

$$P_{\mu}(i) = \frac{\phi_c(i)}{\phi(i)}.$$

In Figure 5, membership probabilities are shown as a function of visual magnitude. The figure shows clear separation of cluster and field stars as sharp distributions of stars around membership values P_{μ} ∼100% and P_{μ} ∼0%. However, due to increasing errors at fainter regime, one can notice a number of stars with intermediate values of P_{μ}, for magnitudes fainter than V=18 mag. The histogram of membership probabilities for 8322 stars is shown in Figure 6. The presence of higher peaks for the leftmost and rightmost bins suggest that the method used for the membership determination is effective for NGC 3201. We find 5981 stars that have membership probabilities larger than 80%. The spatial distribution of the stars is shown in Figure 7. To distinguish between the cluster members and field stars, we have used different symbols for stars having P$_{\mu}$ > 80%, 10% < P_{μ} ≤ 80% and P$_{\mu}$ ≤ 10%. The cut off values of P$_{\mu}$ are based on the histogram shown in Figure 6.

Figure 8 presents the CMD of stars having P$_{\mu}$ > 80%. In this CMD, cluster sequences for stars brighter than $V \sim 20$ mag can be seen. Also, this CMD shows stars of various evolutionary stages like sub-giants, red giants, horizontal branch stars and blue stragglers. All the cluster sequences in this CMD look cleaner with minimal field contamination. As mentioned earlier, NGC 3201 shows differential reddening, due to which the cluster sequences are broadened in CMD. As discussed by Kravtsov et al. (2009), the red giant branch of the cluster, in particular, shows significant broadening. In addition to this, we find gaps in the red giant branch at V ∼13 and V ∼15, the former one being more significant. These gaps have been reported by Lee (1977) in his photometric study of NGC 3201. The horizontal branch of NGC 3201 is well developed and extended, with a relatively unclear instability strip.

3.1. Comparison with Zl12

The PMs presented in this study were compared with the catalogue given by Zl12. For comparison, we plotted the spatial distributions of our catalogue with Zl12 in Figure 9. In this figure, our catalogue stars are shown with red filled circles, while Zl12 stars are shown with blue triangles. It is clearly seen in the figure that the present investigation extends the PM studies of NGC 3201 to a wider region. In the additional observed area in our catalogue, we have PM information from about 2000 stars. For the common stars, the differences in both PM components between the two catalogues is shown in Figure 10. Values of the 3σ-clipped median of the proper motion differences are 0.04(σ = 0.54) mas yr^{-1} and −0.05(σ = 0.62) mas yr^{-1}. Our PMs exhibit consistency with the Zl12 data for $V < 20$ mag.

4. Membership of variables and X-ray sources

We used the membership catalogue to ascertain the membership status of the reported variable stars and X-ray sources in the region of NGC 3201. The details of the comparison are listed in Table 3. The variable stars of NGC 3201 have been compiled on Clement's webpage of the catalogue of variable stars in globular clusters[6]. Recently, some new variable were detected by Kaluzny et al. (2016). We found four variable stars in com-

[6]http://www.astro.utoronto.ca/∼cclement/cat/C1015m461

Table 3: Membership probability of the known variables (ID_V) in the direction of NGC 3201 and X-ray sources from Webb et al. (2006) (ID_X). Star number in our catalogue is denoted by ID.

Variables			X-ray sources		
ID_V	P_μ (%)	ID	ID_X	P_μ (%)	ID
V71	0	3373	22	100	8134
V92	100	5147	25	2	6766
V98	100	4921	26	100	6374
V137	6	7804	30	0	1963
			33	0	624
			45	99	8222
			46	1	3222
			48	77	702
			58	100	7888
			59	98	1229

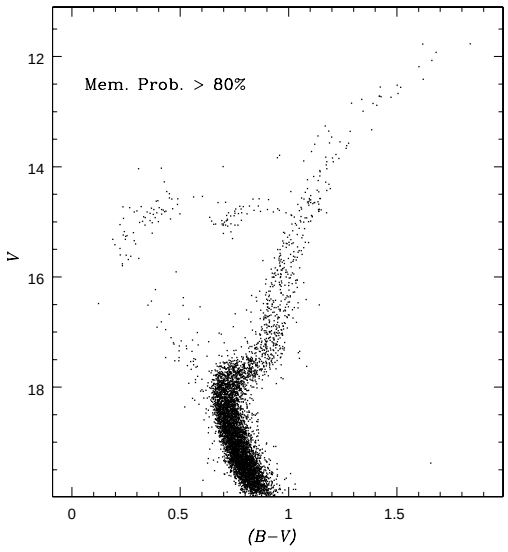

Fig. 8.— V vs. $(B-V)$ CMD for the stars with membership probabilities $> 80\%$

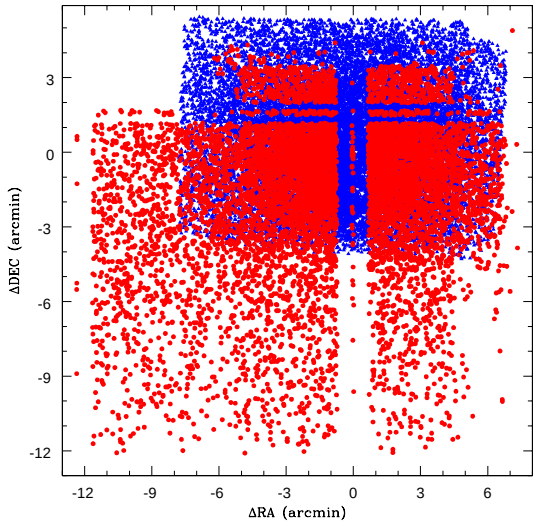

Fig. 9.— Spatial distribution of stars in the present and Zl12 catalogues. Axes shown here are the differences in coordinates of NGC 3201 stars and the cluster center in arcmin. Red filled circles show the present catalogue while blue triangles represent the catalogue of Zl12.

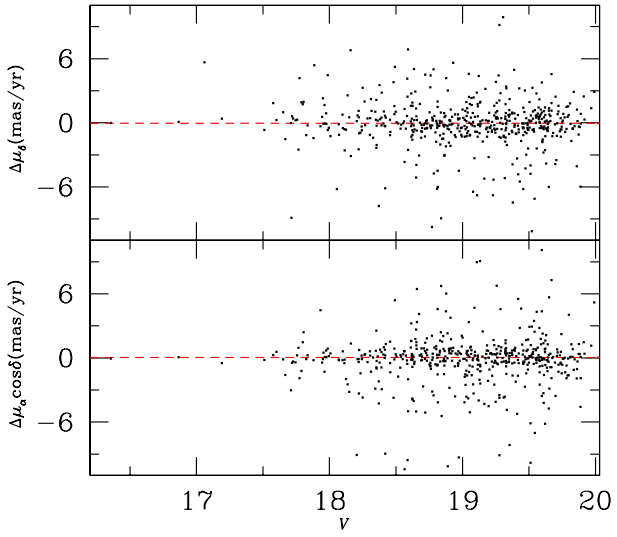

Fig. 10.— Difference between the Zl12 proper motions and those derived in the present study, plotted against visual magnitude. 3σ-clipped median PM differences are shown by the horizontal dashed lines.

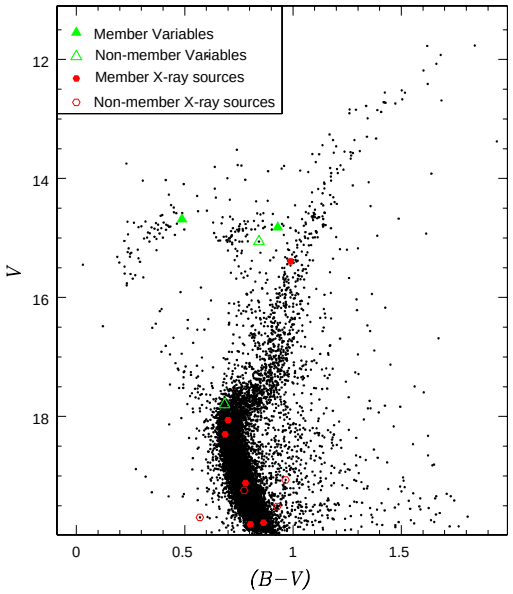

Fig. 11.— The variable stars and X-ray sources found in our membership catalogue are shown in this CMD with different symbols as indicated in the inset. Filled circles and filled triangles show the most probable cluster members, while the open circles and open triangles show the kinematic non-members. This CMD represents all the stars for which membership probabilities have been calculated.

mon with our catalogue. In Table 3, V137 comes from the variables listed in Kaluzny et al. (2016) and the coordinates of the other three variables have been taken from Clement's webpage. As can be seen in Table 3, variables V92 and V98 have a 100% probability of being cluster stars. The two other variable stars, V71 and V137 have P_μ∼0%, which implies that they are not cluster members. The X-ray sources in the NGC 3201 field-of-view have been identified by Webb et al. (2006). Out of 10 X-ray sources found, five sources (ID$_X$= 22, 26, 45, 58, 59) have membership probability close to 100%, which makes them most probable cluster members. Another X-ray source, ID$_X$= 48 should also be a probable cluster member based on its membership probability. ID$_X$= 25, 30, 33, 46 have P_μ∼0%, which means they do not belong to NGC 3201. Figure 11 shows the CMD of all the stars listed in our membership catalogue with the variables and X-ray sources shown with different symbols.

5. The catalogue

The electronic catalogue from the present study contains relative PMs, PM errors, membership probabilities, photometric magnitudes in B, V, I bands with rms errors for 8322 stars in the direction of NGC 3201. Column (1) of the catalogue gives the running number; Columns. (2) and (3) present the J2000.0 equatorial coordinates, while Columns. (4) and (5) show positions of the stars (X and Y) in CCD pixels. Relative PMs and PM errors are listed in Columns. (6) to (9). Columns (10) to (15) provide photometric B, V and I magnitudes and their rms errors. Final Column, column number (16) represent the membership probability P_μ. Some initial lines from the electronic catalogue are shown in Table 4.

6. Conclusions

We provide proper motions and membership probabilities for 8322 stars in the field of globular cluster NGC 3201. Our PMs successfully separate field stars from cluster members, and we present a CMD which shows cluster sequences almost free from field stars. An electronic catalogue with equatorial coordinates, PMs, membership probability and BVI photometry is being made available to the astronomical community. The membership catalogue has been used to define the membership status of variable stars and X-ray sources earlier reported in the cluster's direction. This work also demonstrates that CCD data with only few years epoch gap can provide proper motions accurate enough for kinematic separation of cluster members.

We are indebted to an anonymous referee for a careful reading of the manuscript and giving very useful suggestions which greatly improved this article including its language and presentation. Devesh P. Sariya and Ing-Guey Jiang acknowledge the grant from Ministry of Science and Technology (MOST), Taiwan. The grant numbers are MOST 103-2112-M-007-020-MY3, MOST 104-2811-M-007-024, and MOST 105-2811-M-007 -038. This research used the facilities of the Canadian Astronomy Data Centre operated by the National Research Council of Canada with the support of the Canadian Space Agency. We have also used the catalogue of variable stars managed by Prof. Christine Clement from University of Toronto, Canada.

REFERENCES

Anderson, J., Bedin, L. R., Piotto, G., Yadav, R. K. S., Bellini, A., 2006, A&A, 454, 1029, [A06]

Alcaino, G., 1976, A&AS, 26, 251

Alcaino, G., Liller, W., 1981, AJ, 86, 1480

Alcaino, G., Liller, W., Alvarado, F., 1989, A&A, 216, 68

Anguiano, B., Zucker, D. B., Scholz, R.-D., Grebel, E. K. et al., 2015, MNRAS, 451, 1229

Anguiano, B., De Silva, G. M., Freeman, K., Da Costa, G. S. et al., 2016, MNRAS, 457, 2078

Arellano Ferro, A., Ahumada, J. A., Calderón, J. H., Kains, N., 2014, Rev. Mex. Astron. Astrofis., 50, 307

Balaguer-Núñez, L., Tian, K. P., Zhao, J. L., 1998, A&AS, 133, 387

Bellini, A., Piotto, G., Bedin, L. R., et al., 2009, A&A, 493, 959

Table 4: The membership catalogue for NGC 3201 (initial few lines).

ID	α_{2000}	δ_{2000}	X	Y	$\mu_\alpha cos(\delta)$	$\sigma_{\mu_\alpha cos(\delta)}$	μ_δ	σ_{μ_δ}	B	σ_B	V	σ_V	I	σ_I	P_μ
(1)	(2)	(3)	(4)	(5)	(6)	(7)	(8)	(9)	(10)	(11)	(12)	(13)	(14)	(15)	(16)
	[h:m:s]	[d:m:s]	[pixel]	[pixel]	[mas/yr]	[mas/yr]	[mas/yr]	[mas/yr]	[mag]	[mag]	[mag]	[mag]	[mag]	[mag	[%]
1	10:17:43.87	-46:36:49.1	2535.4886	247.4757	10.9367	0.7142	2.9779	0.3006	17.4382	0.0044	16.6389	0.0045	15.7423	0.0052	0
2	10:17:17.45	-46:36:50.5	3681.3510	247.7929	-0.6062	1.0181	1.4117	0.1478	18.8624	0.0022	18.1265	0.0017	17.2219	0.0008	0
3	10:16:54.53	-46:36:49.9	4675.0902	254.5138	14.3016	0.8902	0.8736	1.3054	17.4766	0.0028	16.5418	0.0061	15.4859	0.0041	0
4	10:17:27.99	-46:36:46.7	3224.0258	261.3223	13.9711	0.8437	6.6451	1.6193	19.7695	0.0055	18.7313	0.0111	17.6100	0.0029	0
5	10:17:06.37	-46:36:44.3	4161.2320	275.8470	14.7467	0.6278	9.3091	0.4916	17.9729	0.0044	16.8013	0.0039	15.4686	0.0024	0
6	10:16:55.80	-46:36:44.2	4619.5001	278.2980	10.9301	0.8520	4.0641	1.6559	20.1599	0.0077	19.1355	0.0094	17.9470	0.0163	0
7	10:17:43.89	-46:36:41.3	2534.5683	279.9379	-0.9899	1.1377	2.5727	0.9101	19.7797	0.0104	18.9841	0.0012	18.0374	0.0085	45
8	10:17:41.74	-46:36:37.4	2627.5263	297.0895	13.4994	1.0762	5.7681	1.3270	19.7509	0.0060	18.6114	0.0076	17.3379	0.0075	0
9	10:17:49.71	-46:36:36.2	2281.8995	299.8237	13.6555	1.1161	1.7871	1.8352	19.1304	0.0055	18.0739	0.0017	16.9377	0.0057	0
10	10:17:22.46	-46:36:31.1	3463.3688	328.1909	13.0958	0.5066	5.6286	0.2441	18.3758	0.0104	17.3988	0.0039	16.3546	0.0008	0
11	10:17:28.71	-46:36:29.1	3192.3215	335.1330	10.8703	1.1676	6.7231	1.3137	18.7126	0.0077	17.8893	0.0138	16.9378	0.0057	0

Brewer, J. P., Fahlman, G. G., Richer, H. B. et al., 1993, AJ, 105, 2158

Casetti-Dinescu, D. I., Girard, T. M., Herrera, D., van Altena, W. F. et al., 2007, AJ, 134, 195

Cacciari, C., 1984a, AJ, 89, 231

Cacciari, C., 1984b, AJ, 89, 1082

Chen, C. W., Chen, W. P., 2010, ApJ, 721, 1790

Chun, M.-S., 1988, The Journal of Korean Astronomical Society, 21, 67

Cote, P., Welch, D. L., Fischer, P., Da Costa, G. S., Tamblyn, P., Seitzer, P., & Irwin, M. J., 1994, ApJ Suppl. Ser., 90, 83

Cote, P., Welch, D. L., Fischer, P., Gebhardt, K., 1995, ApJ, 454, 788

Covey, K. R., Wallerstein, G., Gonzalez, G., Vanture, A. D., Suntzeff, N. B., 2003, PASP, 115, 819

Covino, S., Ortolani, S., 1997, A&A, 318, 40

Cudworth, K. M., 1986, IAUS, 109, 201

Cudworth, K. M., 1997, ASP Conf. Series, 127, 91

Da Costa, G. S., Tamblyn, P., Seitzer, P. et al., 1993, ASP Conf. Ser., 50, 81

Dambis, A. K., 2006, Astronomical and Astrophysical Transactions, 25, 185

Gonzalez, G., Wallerstein, G., 1998, AJ, 116, 765

Harris, W. E., 1996, AJ, 112, 1487

Kaluzny, J., Rozyczka, M., Thompson, I. B., Narloch, W., Mazur, B., Pych, W. et al. 2016, Acta Astronomica, 66, 31

Kravtsov, V., Alcaíno, G., Marconi, G., Alvarado, F., 2009, A&A, 497, 371

Kravtsov, V., Alcaíno, G., Marconi, G. Alvarado, F., 2010, A&A, 512, L6

Kunder, A., Bono, G., Piffl, T., Steinmetz, M. et al., 2014, A&A, 572, A30

Layden, A. C., Sarajedini, A., AJ, 2003, 125, 208

Lee, S.-W., 1977, A&AS, 28, 409

Lee, J-W., Carney B. W., 1999, AJ, 118, 1373

Mazur, B., Krzeminski, W., and Thompson, I. B., 2003, MNRAS, 340, 1205

Menzies, J., 1967, Ph.D. thesis, Australian National University

Muñoz, C., Geisler, D., Villanova, S., 2013, MNRAS, 433, 2006

Mucciarelli, A., Lapenna, E., Massari, D., Ferraro, F. R., and Lanzoni, B., 2015, ApJ, 801, 69

Penny, A.J., 1984, in Observational Tests of the Stellar Evolution Theory, IAU Symp. 105, ed(s). A. Maeder and A. Renzini (Dordrecht:Reidel), 157

Piersimoni, A. M., Bono, G., Ripepi, V., 2002, AJ, 124, 1528

Piotto, G., Bedin, L. R., Cassisi, S., Anderson, J. et al., 2004, Mem. S. A. It. Suppl., 5, 71

Pryor, C., Meylan, G., 1993, ASP Conf. Series, 50, 357

Sanders, W. L., 1971a, A&A, 15, 368

Sanders, W. L., 1971b, A&A, 14, 226

Sariya, D. P., Yadav, R. K. S., Bellini, A., 2012, A&A, 543, A87

Sariya, D. P., Yadav, R. K. S., 2015, A&A, 584, A59

Simmerer, J., Ivans, I. I., Filler, D. et al., 2013, ApJL, 764, L7

Stetson, P. B., 1980, AJ, 85, 387

Tian, K.-P., Zhao, J.-L., Shao, Z.-Y., Stetson, P. B., 1998, A&AS, 131, 89

Vasilevskis, S., Klemola, A., Preston, G., 1958, AJ, 63, 387

von Braun, K., Mateo, M., 2001, AJ, 121, 1522

von Braun, K., Mateo, M. 2002, AJ, 123, 279

Webb, N. A., Wheatley, P. J., Barret, D., 2006, A&A, 445, 155

Yadav, R. K. S., Bedin, L. R., Piotto, G. et al., 2008, A&A, 484, 609

Yadav, R. K. S., Sariya, D. P., Sagar, R., 2013, MNRAS, 430, 3350

Zhao, J. L. & He, Y. P., 1990, A&A, 237, 54

Zhao, J. L. & Shao, Z. Y., 1994, A&A, 288, 89

Zloczewski, K., Kaluzny, J., Rozyczka, M., Krzeminski, W., Mazur, B., 2012, Acta Astronomica, 62, 357

This 2-column preprint was prepared with the AAS LaTeX macros v5.0.